

# Unbiased estimation of sampling variance for Simpson's diversity index

Andreas Tiffreau-Mayer<sup>1</sup>

<sup>1</sup>Division of Infection and Immunity & Institute for the Physics of Living Systems, University College London  
(Dated: October 6, 2023)

Quantification of measurement uncertainty is a cornerstone of scientific inquiry. Yet, for ecological measures of diversity obtaining reliable estimates of this uncertainty is a surprisingly challenging statistical problem. Here, a solution to this problem is presented in the form of an unbiased estimator for the sampling variance of Simpson's diversity index. Numerical tests show that this estimator outperforms currently used methods by large margins in small samples. We illustrate uses of the estimator for quantifying diversity in marine ecology and immunology.

Do measured diversities differ more than expected by chance? When comparing diversities of two samples taken at different times (or different locations), we expect some variability due to finite sampling even if the underlying population has not changed. To reliably compare diversities thus requires statistical tools to quantify this sampling variance [1–6].

Here, we introduce an unbiased estimator of the sampling variance of Simpson's index, a classical ecological measure of species diversity that takes into account both species richness and evenness [1]. The development of this estimator was prompted by our recent work on quantifying the diversity of adaptive immune receptors [7]. In this setting the total number of species  $S$  often exceeds sample sizes  $N$ . Somewhat surprisingly diversity can still be estimated in this regime as coincidences start to occur much before the distribution itself has been fully sampled; a fact closely related to the birthday paradox in probability theory [8, 9] and known in statistical physics as Ma's square-root regime of entropy estimation [2, 10, 11]. However, we show that commonly used methods [3, 4] for estimating the variance of Simpson's diversity index are highly biased in this undersampled regime. The unbiased estimator proposed here alleviates this bias and additionally reduces the variability of estimates compared to alternative methods.

Simpson's index is used widely from ecology [1, 13] and microbiology [4, 14] to economics [15], and has an intuitive interpretation as the probability of species co-incidence when comparing random pairs of individuals. Mathematically, this index is defined as [1],

$$p_C = \sum_{i=1}^S p_i^2, \quad (1)$$

where  $p_i$  is the frequency of species  $i$  in the population  $i = 1, \dots, S$ , where  $S$  is the number of distinct species. Simpson's index can be converted into a true diversity by  $D = 1/p_C$ , where the true diversity (or Hill number) is an effective number of equally abundant species that would have the same diversity index [13]. The negative logarithm of Simpson's index,  $-\log p_C$ , is the Renyi entropy (of order 2) [6, 16]. Furthermore, Shannon entropy  $-\sum_i p_i \log p_i$  is lower bounded by  $-\log p_C$ , a relation

that has been exploited to estimate entropy rates of dynamical systems [2, 10] and neural spike trains [17].

To illustrate how this index can be applied consider the following question: Has climate change led to a biodiversity loss in the Mediterranean sea? To answer this question Albano et al. [12] counted the number  $n_i$  of molluscs belonging to species  $i$  in a patch of the sea floor and also performed the same count for empty mollusc shells found at the same site in death assemblages. Simpson's diversity index turns the species abundance distributions (Fig. 1A) into scalar measures of current and past biodiversity (points in Fig. 1B). As Simpson's index needs to be estimated from sampled counts  $n_i$  (instead of the unknown population frequencies  $p_i$ ) it will vary even between replicate samples from the same population. The method introduced here allows the quantification of this

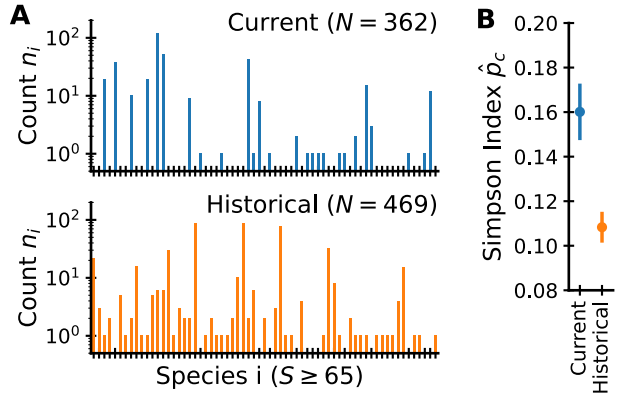


FIG. 1: Illustration of the problem setting with data from marine ecology: quantifying uncertainty in estimating diversity from finite samples. (A) Distributions of sampled mollusc species currently alive (top) and found in surficial dead assemblages (bottom). We consider the problem of how to summarize each distribution into a diversity statistic with associated sampling uncertainty interval. (B) Simpson Diversity index with error bars calculated using the proposed method (Eq. 16). Error bars show  $\hat{p}_C \pm \sqrt{\hat{\text{Var}}_{\text{unbiased}}(\hat{p}_C)}$ . Data: Non-invasive mollusc species found on shallow subtidal ground at 12m depth of the coast of Ashqelon in the Eastern Mediterranean sea [12].

sampling variability (bars in Fig. 1B). It thus allows us to conclude that the increase in Simpson's index relative to past levels is larger than expected by chance, hence that biodiversity ( $= 1/p_C$ ) has decreased significantly.

More formally, in a sample of size  $N$  the distribution of counts  $n_i$  follows a multinomial distribution with probabilities  $p_i$ ,

$$P(n_1, \dots, n_S) = \frac{N!}{\prod_{i=1}^S n_i!} \prod_{i=1}^S p_i^{n_i}, \quad (2)$$

with  $\sum_i n_i = N$ . To estimate  $p_C$  from a sample, it is tempting to simply replace the population frequencies  $p_i$  in Eq. 1 with the sampled frequencies  $f_i = n_i/N$ . However, one is well advised to resist this temptation as such plugin estimators are known to be severely biased in small samples [1–3, 18]. To obtain an unbiased estimate of  $p_C$  Simpson [1] demonstrated that the probability of coincidence when subsampling without replacement,

$$\hat{p}_C = \frac{\sum_{i=1}^S n_i(n_i - 1)}{N(N - 1)}, \quad (3)$$

provides the correct measure. For the following derivations it is instructive to prove that this estimator is indeed unbiased, i.e.  $\langle \hat{p}_C \rangle = p_C$ , where  $\langle \cdot \rangle$  is an average over repeated samples of a fixed size. Evaluating the expectation requires calculating the factorial moment  $\langle n_i(n_i - 1) \rangle$ , which can be calculated most conveniently from the probability generating function  $G(z_1, \dots, z_S) = \langle \prod_i z_i^{n_i} \rangle$ . From the definition of  $G$  it directly follows that  $\frac{\partial}{\partial z_i^2} G(1, \dots, 1) = \langle n_i(n_i - 1) \rangle$ . For the multinomial distribution  $G(z_1, \dots, z_S) = (\sum_i p_i z_i)^N$ , and thus

$$\langle n_i(n_i - 1) \rangle = N(N - 1)p_i^2. \quad (4)$$

This result shows that Eq. 3 is an unbiased estimator of  $p_C$ ,

$$\langle \hat{p}_C \rangle = \frac{\sum_i \langle n_i(n_i - 1) \rangle}{N(N - 1)} = p_C. \quad (5)$$

Simpson furthermore gave an expression for the sampling variance of this estimator (derived in the appendix for completeness),

$$\text{Var}(\hat{p}_C) = ap_T - bp_C^2 + cp_C, \quad (6)$$

which is a linear combination of the triplet coincidence probability

$$p_T = \sum_{i=1}^S p_i^3, \quad (7)$$

the squared coincidence probability  $p_C^2$ , and the coincidence probability  $p_C$ , with sample size dependent parameters

$$a = \frac{4(N - 2)}{N(N - 1)}, \quad b = \frac{2(2N - 3)}{N(N - 1)}, \quad c = \frac{2}{N(N - 1)}. \quad (8)$$

A simple way to estimate this variance from a finite sample is to plug the empirical species frequencies  $f_i$  into Eq. 6 in place of the population probabilities  $p_i$ ,

$$\hat{\text{Var}}_{\text{plugin}} = a \sum_{i=1}^S f_i^3 - b \left( \sum_{i=1}^S f_i^2 \right)^2 + c \sum_{i=1}^S f_i^2. \quad (9)$$

However, we will find that this plugin estimator is substantially biased for small  $N$ , similarly to plugin estimators of diversity indices themselves.

To derive a better estimator we exploit the linearity of Eq. 6 and decompose the problem into the unbiased estimation of each of the three terms. For the first term, the analogy to  $\hat{p}_C$  suggests to estimate the triplet probability as

$$\hat{p}_T = \frac{\sum_{i=1}^S n_i(n_i - 1)(n_i - 2)}{N(N - 1)(N - 2)}. \quad (10)$$

To show that this estimator is unbiased, requires calculating the third factorial moment  $\langle n_i(n_i - 1)(n_i - 2) \rangle$ . In analogy to Eq. 4 this factorial moment can again be calculated taking derivatives of the probability generating function  $G$  of the multinomial distribution,

$$\langle n_i(n_i - 1)(n_i - 2) \rangle = \frac{\partial^3 G(1, \dots, 1)}{\partial z_i^3} \quad (11)$$

$$= N(N - 1)(N - 2)p_i^3. \quad (12)$$

This result shows that  $\hat{p}_T$  is unbiased,

$$\langle \hat{p}_T \rangle = \frac{\sum_i \langle n_i(n_i - 1)(n_i - 2) \rangle}{N(N - 1)(N - 2)} = p_T. \quad (13)$$

For the second term, we re-express the squared coincidence probability as

$$p_C^2 = \langle \hat{p}_C^2 \rangle - \text{Var}(\hat{p}_C). \quad (14)$$

where we have used the variance decomposition formula,  $\text{Var}(\hat{p}_C) = \langle \hat{p}_C^2 \rangle - \langle \hat{p}_C \rangle^2$ , and the unbiasedness of Simpson's estimator,  $\langle \hat{p}_C \rangle = p_C$ . Plugging this expression into Eq. 6 and solving for  $\text{Var}(\hat{p}_C)$  we obtain

$$\text{Var}(\hat{p}_C) = \frac{a}{1 - b} p_T - \frac{b}{1 - b} \langle \hat{p}_C^2 \rangle + \frac{c}{1 - b} p_C. \quad (15)$$

Finally, Eq. 3 provides an unbiased estimate for the third term as shown by Simpson [1]. We thus have all components in place for our central result,

$$\hat{\text{Var}}_{\text{unbiased}}(\hat{p}_C) = \frac{a}{1 - b} \hat{p}_T - \frac{b}{1 - b} \langle \hat{p}_C^2 \rangle + \frac{c}{1 - b} \hat{p}_C, \quad (16)$$

is an unbiased estimator for  $\text{Var}(\hat{p}_C)$ .

To compare the empirical performance of this estimator with other proposals we turned to numerical experiments. We generated a random probability distribution of support  $S = 1000$  by sampling  $p_i$  uniformly from the

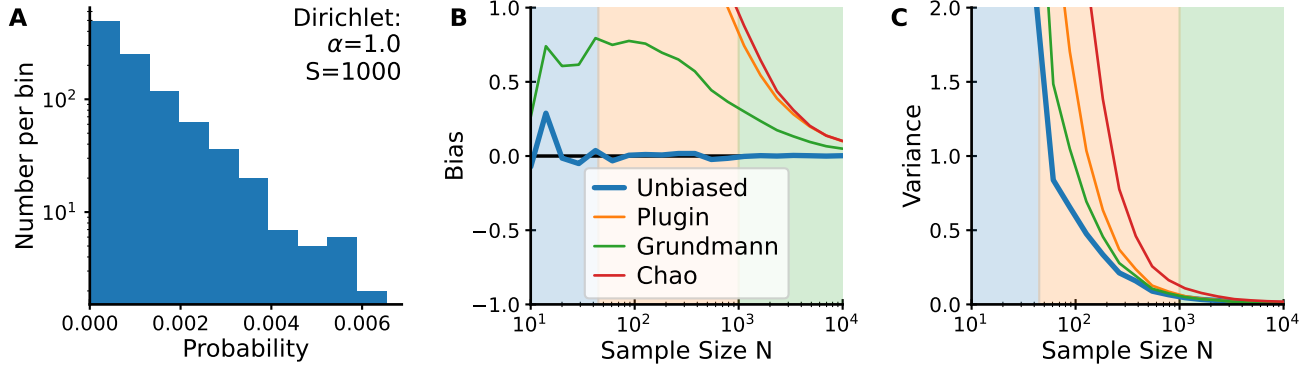


FIG. 2: **Benchmarking of variance estimators on simulated data.** (A) Histogram of species abundances in the simulated distribution. Probabilities of  $S = 1000$  species were drawn from a Dirichlet distribution of parameter  $\alpha = 1$ . (B) Bias and (C) variance as a function of sample size  $N$ . Expectation values were calculated over 1000 repeated draws at each sample size from the population distribution. Bias and variance are expressed as fractions, i.e. divided by the true value or its square, respectively. The shaded areas differentiate sampling regimes: blue  $N < \sqrt{2S}$ , orange  $\sqrt{2S} < N < S$ , and green  $N > S$ .

probability simplex, this is from a Dirichlet distribution,  $\rho(p_i) \propto p_i^{\alpha-1}$ , with  $\alpha = 1$  (Fig. 2A). We next simulates drawing samples of different sizes  $N$  ranging from  $N = 10$  to  $N = 10000$  from the population. Repeated sampling at a given sample size allows evaluation of how empirical estimates deviate from the ground truth value,  $\text{Var}(\hat{p}_C)$ , computed using Eq. 6 from the species abundances.

Given an estimator  $\hat{x}$  of a parameter with true value  $x$  a natural measure of its quality is the mean squared error,

$$\text{MSE}(\hat{x}) = \langle (\hat{x} - x)^2 \rangle, \quad (17)$$

which can be decomposed into a bias and variance term,

$$\text{MSE}(\hat{x}) = \text{Bias}(\hat{x})^2 + \text{Var}(\hat{x}), \quad (18)$$

where  $\text{Bias}(\hat{x}) = \langle \hat{x} - x \rangle$  and  $\text{Var}(\hat{x}) = \langle (\hat{x} - \langle \hat{x} \rangle)^2 \rangle$ . To make the values more readily interpretable we normalize Bias and Variance by the true value  $x$  to the fractional values,  $\text{Bias}/x$  and  $\text{Var}/x^2$ . We display bias (Fig. 2B) and variance (Fig. 2C) separately, to investigate any potential trade-offs between bias and variance [19].

The numerical results demonstrate that the proposed estimator is not only unbiased (Fig. 2B), but also has lower variance than all other estimators (Fig. 2C). For sample sizes  $N > S$  (green shading) all estimators have relatively low variance, but alternative estimators are substantially biased unless  $N \gg S$ . All estimators are highly variable for very small sample sizes  $N < \sqrt{2S}$  (blue shading), which corresponds to the sample size at which the expected number of coincidences in a uniform distribution of  $S$  species is one.

In addition to the plugin estimator (Eq. 9), we compared our estimator against two state of the art methods introduced by Grundmann et al. [4] and Chao et al. [3].

Grundmann's method consists in plugging the empirical frequencies into an asymptotic expansion of Eq. 6 for  $N \rightarrow \infty$ ,

$$\hat{\text{Var}}_{\text{Grundmann}}(\hat{p}_C) = \frac{4}{N} \left( \sum_{i=1}^S f_i^3 - \left( \sum_{i=1}^S f_i^2 \right)^2 \right). \quad (19)$$

Chao's method estimates variances by bootstrapping from a population constructed from the sample by coverage-reweighting observed species frequencies and by augmenting the sample with an estimated number of rare unseen species. The number of bootstrap samples was set to 200 as recommended by Chao et al. [3]. This method is widely used in the field due to its implementation in the popular R package iNEXT [21]. Surprisingly, despite its widespread use, we find that this estimator has the largest bias and variance of tested methods.

To test the generality of our findings, we repeated the numerical experiments with alternative species distributions. First, we generated a more peaked and more uniform distribution of species abundances by drawing species abundance distributions from a Dirichlet distribution with parameter  $\alpha = 0.25$  and  $\alpha = 4$ , respectively. The results demonstrate that the unbiased estimator consistently performs best regardless of the choice of  $\alpha$  (Fig. S1). Second, we tested the estimators on a heavy-tailed distribution. We chose probabilities of species according to Zipf's law, in which the probability of the  $i$ th most abundant species is  $p_i \sim 1/i$ . The results again show that other methods can have substantial bias in small samples that is removed by the proposed unbiased estimator (Fig. S2).

We also compared estimators on a real-world problem: the estimation of T cell receptor (TCR) diversity. Stochastic genetic recombination creates hypervariable

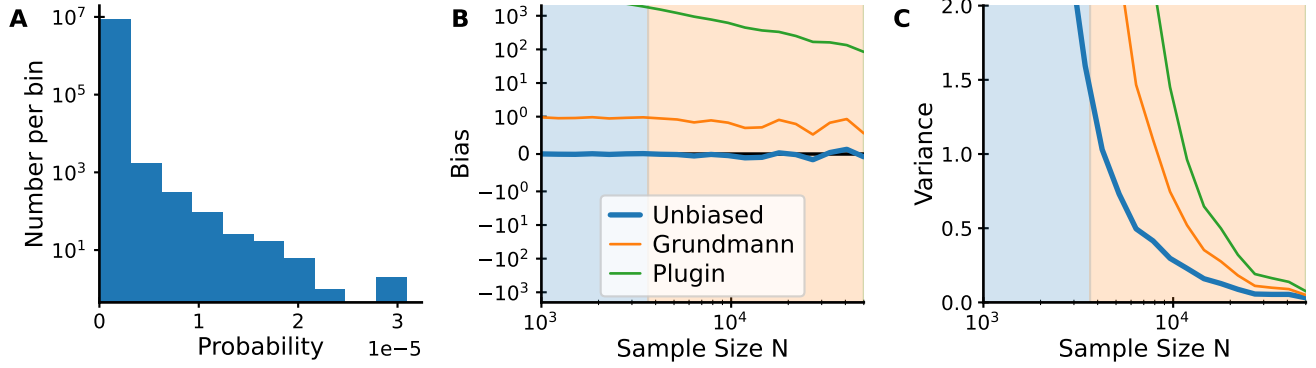


FIG. 3: **Benchmarking of variance estimators on T cell receptor repertoire data.** (A) Histogram of CDR3 $\beta$  multiplicities among ten million TCR sequences generated by OLGA [20]. (B) Bias and (C) variance as a function of sample size  $N$ . Expectation values were calculated at each sample size by splitting the total sequence pool into non-overlapping subsets. Bias and variance are expressed as fractions, i.e. divided by the true value or its square, respectively. The shaded areas differentiate sampling regimes: blue  $N < \sqrt{2D}$ , orange  $\sqrt{2D} < N$  with true diversity  $D = 1/p_C \sim 7 \cdot 10^6$  (estimated by applying Eq. 3 to all generated sequences). Note that in (B) a logarithmic scale is used for absolute values larger than 1 to account for the large bias of the plugin method.

TCRs, which are the molecular basis for how our adaptive immune system responds to diverse pathogens [22]. TCR diversity can be quantified by considering receptors as "species" with associated probabilities corresponding to how likely each sequence is created by recombination. We used a computational model of recombination called OLGA [20] to generate  $10^7$  sequences using the default human TCR $\beta$ -model, and determined the uncertainty of diversity estimates for the hypervariable complementary determining region 3 (CDR3) at different sample sizes. The unbiased estimator substantially outperforms other benchmarked estimators (Fig. 3), which are very substantially biased. (Chao's estimator was excluded from this comparison due to its slow computational speed at tested sample sizes.) The estimation of TCR diversity is an interesting benchmark for variance estimators in the undersampled regime: The number  $S$  of receptors that can be created by recombination is immense with estimates as large as  $S \sim 10^{39}$  for the TCR $\beta$  chain [23]. Our ability to estimate Simpson's diversity from samples of only  $N \sim 10000$  cells, i.e. for  $N < \sqrt{2S}$ , is surprising. It hinges on the wide distribution of TCR generation probabilities [20], which makes the effective diversity  $D = 1/p_C \sim 7 \cdot 10^6$  much smaller than  $S$ .

To gain intuition into how estimator performance depends on  $N$  it is instructive to consider limits of the variance formula (Eq. 6). For large  $N$ , the variance is asymptotically equal to

$$\text{Var}(\hat{p}_C) = \frac{4}{N} \left( \sum_i p_i^3 - \left( \sum_i p_i^2 \right)^2 \right). \quad (20)$$

This implies that in large samples the variance of the estimator scales with the familiar  $1/N$  scaling of an arith-

metic average. Note further that the expression in brackets can be interpreted as the variance of species probabilities,  $\text{Var}(p) = \langle p^2 \rangle - \langle p \rangle^2 = p_T - p_C^2$ . Estimating this variance from empirical frequencies leads to additional sampling variance, which explains why plugin estimators are positively biased. Conversely, when the number of species  $S$  is increased at fixed  $N$  the third term in Eq. 6 asymptotically dominates as  $p_T \sim 1/S^2$  and  $p_C^2 \sim 1/S^2$  while  $p_C \sim 1/S$ , thus

$$\text{Var}(\hat{p}_C) = \frac{2}{N(N-1)} p_C. \quad (21)$$

Interestingly, here the variance scales as  $1/N^2$ , which explains the sharp rise in variances as  $N \sim \sqrt{2S}$ . As coincidences are rare in this limit they occur roughly independently across the  $N(N-1)/2$  pairs of individuals, and the distribution of the total number of coincidences  $n_C$  is approximately Poissonian [24] with mean  $\langle n_C \rangle = N(N-1)p_C/2$ . The variance of a Poisson distribution equals its mean, and as  $\hat{p}_C = \frac{2n_C}{N(N-1)}$  we have  $\text{Var}(\hat{p}_C) = \frac{4}{N^2(N-1)^2} \langle n_C \rangle = \frac{2}{N(N-1)} p_C$ . A Poisson approximation thus recovers Eq. 21 and the scaling is inversely quadratic as the number of pairs grows quadratically with sample size.

As a final application example, we return to the quantification of TCR diversity. Only a small fraction of all possible receptors bind to any given molecular target, a peptide presented on a major histocompatibility complex (pMHC). Recent experimental advances in single cell sequencing of sorted T cell populations stained with multimerized pMHC tetramers have given us a view onto the diversity of TCRs that can engage a given target [25–27], but the relatively small numbers of only a few hun-

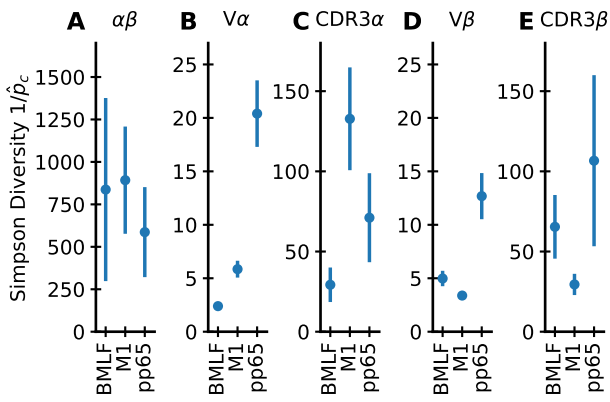


**FIG. 4: Quantifying the diversity of epitope-specific T cell receptors.** Data from Dash et al. [25] of three groups of receptors each recognizing a different viral epitope. The  $\alpha\beta$  TCR is a heterodimer composed of an  $\alpha$  and  $\beta$  chain, each of which specified by the choice of a V gene and the primary amino acid sequence of the hypervariable CDR3 region. The diversity of pMHC-specific receptor can be determined for (A) the full receptor, this is the  $V\alpha$ -CDR3 $\alpha$ - $V\beta$ -CDR3 $\beta$  sequence, and separately for (B) the  $V\alpha$  gene choice, (C) the CDR3 $\alpha$  sequence, (D) the  $V\beta$  gene choice, and (E) the CDR3 $\beta$  sequence.

dred cells per target recovered in these experiments has complicated precise quantification. Here, we apply our estimator to quantify sampling uncertainty. The dataset consists of 415 paired chain TCR $\alpha\beta$  receptors, specific against three pMHCs [25]: the Epstein-Barr virus epitope BMLF<sub>1-280</sub> presented on HLA-A\*02:01 (BMLF), the human cytomegalovirus epitope pp65<sub>495</sub> presented on HLA-B\*07:02 (pp65), and the influenza virus epitope M1<sub>58</sub> presented on HLA-A\*02:01 (M1). Each experiment involved sorting T cells from multiple individuals, but for simplicity we will determine overall TCR diversity regardless of donor-origin, a limitation which can be relaxed in the future as dataset sizes increase.

Using our method we determined diversity of the full receptor (Fig. 4A) and its parts (Fig. 4B-E) along with their associated sampling variances. For simplicity true diversities are shown,  $D = 1/\hat{p}_C$ , with error bars calculated by error propagation  $\sqrt{\text{Var}(\hat{p}_C)/\hat{p}_C^2}$ . The results show that overall diversity is highly restricted to the order of a thousand  $\alpha\beta$ TCRs (Fig. 4A). Interestingly, among pMHC-specific groups there are significant differences in  $\alpha$  and  $\beta$  chain diversity (Fig. 4B-E). For instance, M1-specific TCRs have significantly less diverse  $\beta$  chains than  $\alpha$  chains, while the reverse is true for BMLF-specific TCRs. V gene diversity also significantly differs between epitopes, and is largest among pp65-specific TCRs. Taken together this quantification provides statistical evidence for hypothesized differences [25, 27] of  $\alpha$  and  $\beta$  chain diversity between epitope-specific reper-

toires. Importantly, quantification of TCR diversity at different levels leads to testable hypotheses concerning the structural basis of recognition. One might be predicted, for example, that pp65-specific TCRs make fewer contacts between the V-gene encoded CDR1 and CDR2 loops and the pMHC. Similarly, the low CDR3 $\beta$  diversity of M1-specific TCRs predicts that this loop might make many contacts with its cognate pMHC.

In summary, this work describes how the sample variance of Simpson's diversity index can be estimated without bias. Somewhat surprisingly, this unbiased estimator does not seem to be widely known despite its superior properties than alternative proposals. Additionally the unbiased estimator has a closed form analytical expression and is thus fast to calculate even for large samples, in contrast to bootstrapping approaches. To aid adoption of the method we have made a reference open source implementation of the estimator available as a Python package [28]. Improved methods for estimating confidence intervals for diversity metrics are expected to enable better focusing of sampling efforts when monitoring biodiversity in our changing world.

**Acknowledgements.** The author thanks Curtis G. Callan and Yuta Nagano for critical reading of the manuscript. The work was supported in parts by the Royal Free Charity and was concluded at the Aspen Center for Physics, which is supported by National Science Foundation grant PHY-2210452.

---

- [1] E. H. Simpson, *Nature* **163**, 688 (1949).
- [2] I. Nemenman, F. Shafee, and W. Bialek, in *Advances in Neural Information Processing Systems*, edited by T. Dietterich, S. Becker, and Z. Ghahramani (MIT Press, 2001), vol. 14.
- [3] A. Chao, N. J. Gotelli, T. C. Hsieh, E. L. Sander, K. H. Ma, R. K. Colwell, and A. M. Ellison, *Ecological Monographs* **84**, 45 (2014).
- [4] H. Grundmann, S. Hori, and G. Tanner, *Journal of Clinical Microbiology* **39**, 4190 (2001).
- [5] B. Haegeman, J. Hamelin, J. Moriarty, P. Neal, J. Dushoff, and J. S. Weitz, *The ISME Journal* **7**, 1092 (2013).
- [6] M. Roswell, J. Dushoff, and R. Winfree, *Oikos* **130**, 321 (2021).
- [7] A. Mayer and C. G. Callan, Jr, *Proc. Natl. Acad. Sci. U.S.A.* **120**, e2213264120 (2023).
- [8] T. S. Nunnikoven, *American Statistician* **46**, 270 (1992).
- [9] L. Paninski, *IEEE Transactions on Information Theory* **54**, 4750 (2008).
- [10] S.-k. Ma, *Journal of Statistical Physics* **26** (1981).
- [11] D. G. Hernández, A. Roman, and I. Nemenman, *Physical Review E* **108**, 014101 (2023).
- [12] P. G. Albano, J. Steger, M. Bošnjak, B. Dunne, Z. Galfaró, E. Turapova, Q. Hua, D. S. Kaufman, G. Rilov, and M. Zuschin, *Proceedings of the Royal Society B: Biological Sciences* **288**, 20202469 (2021).

- [13] L. Jost, *Oikos* **113**, 363 (2006).
- [14] P. R. Hunter and M. A. Gaston, *Journal of Clinical Microbiology* **26**, 2465 (1988).
- [15] J. P. Gibbs and W. T. Martin, *American Sociological Review* **27**, 667 (1962).
- [16] S. Xu, L. Böttcher, and T. Chou, *Physical Biology* **17**, 031001 (2020).
- [17] S. P. Strong, R. Koberle, R. de Ruyter van Steveninck, and W. Bialek, *Physical Review Letters* **80**, 197 (1998).
- [18] P. Grassberger, arXiv preprint arXiv:0307138 pp. 1–5 (2003).
- [19] P. Mehta, M. Bukov, C.-H. Wang, A. G. R. Day, C. Richardson, C. K. Fisher, and D. J. Schwab, *Physics Reports* **810**, 1 (2019).
- [20] Z. Sethna, Y. Elhanati, C. G. Callan, A. Walczak, and T. Mora, *Bioinformatics* **35**, 2974 (2019).
- [21] T. C. Hsieh, K. H. Ma, and A. Chao, *Methods in Ecology and Evolution* **7**, 1451 (2016).
- [22] A. Mayer, V. Balasubramanian, T. Mora, and A. M. Walczak, *Proc. Natl. Acad. Sci. U.S.A.* **112**, 5950 (2015).
- [23] T. Mora and A. Walczak, in *Systems Immunology*, edited by J. Das and C. Jayaprakash (CRC Press, 2019), chap. 11.
- [24] D. Aldous, *Probability Approximations via the Poisson Clumping Heuristic*, vol. 77 of *Applied Mathematical Sciences* (Springer, New York, NY, 1989).
- [25] P. Dash, A. J. Fiore-Gartland, T. Hertz, G. C. Wang, S. Sharma, A. Souquette, J. C. Crawford, E. B. Clemens, T. H. Nguyen, K. Kedzierska, et al., *Nature* **547**, 89 (2017).
- [26] J. Glanville, H. Huang, A. Nau, O. Hatton, L. E. Wagar, F. Rubelt, X. Ji, A. Han, S. M. Kram, C. Pettus, et al., *Nature* **547**, 94 (2017).
- [27] A. A. Minervina, M. V. Pogorelyy, A. M. Kirk, J. C. Crawford, E. K. Allen, C. H. Chou, R. C. Mettelman, K. J. Allison, C. Y. Lin, D. C. Brice, et al., *Nature Immunology* **23**, 781 (2022).
- [28] <https://github.com/andim/pydiver>

## Appendix: Derivation of the variance expression

To derive the variance of Simpson's estimator we need to calculate various (cross-)moments of the multinomial distribution. Taking derivatives of the probability generating function demonstrates that

$$\left\langle \prod_i n_i^{(a_i)} \right\rangle = N^{\left(\sum_i a_i\right)} \prod_i p_i^{a_i}, \quad (22)$$

where  $x^{(n)} = x(x-1)\dots(x-n+1)$  denotes a falling factorial. The raw moments of the distribution can be

expressed in terms of the factorial moments using Stirling numbers. Alternatively, they can be directly calculated from the moment generating function,

$$M(t_1, \dots, t_S) = G(e^{t_1}, \dots, e^{t_S}) = \langle e^{\sum_i t_i n_i} \rangle, \quad (23)$$

which for the multinomial distribution is equal to

$$M(t_1, \dots, t_S) = \left( \sum_i p_i e^{t_i} \right)^N. \quad (24)$$

Calculating the partial derivatives of the moment generating function at  $t_1 = \dots = t_S = 0$  we obtain

$$\langle n_i \rangle = N p_i \quad (25)$$

$$\langle n_i^2 \rangle = N^{(2)} p_i^2 + N p_i \quad (26)$$

$$\langle n_i^3 \rangle = N^{(3)} p_i^3 + 3N^{(2)} p_i^2 + N p_i \quad (27)$$

$$\langle n_i^4 \rangle = N^{(4)} p_i^4 + 6N^{(3)} p_i^3 + 7N^{(2)} p_i^2 + N p_i. \quad (28)$$

The variance of  $\hat{p}_C$  can be expressed as

$$\text{Var}(\hat{p}_C) = \frac{\langle (\sum_i n_i(n_i - 1))^2 \rangle}{(N(N-1))^2} - p_C^2. \quad (29)$$

The key calculation concerns the numerator of the first term, which is equal to

$$\sum_i \langle (n_i^{(2)})^2 \rangle + \sum_i \sum_{j \neq i} \langle n_i^{(2)} n_j^{(2)} \rangle \quad (30)$$

Expanding the first term, and evaluating the second average using Eq. 22 yields

$$\sum_i (\langle n_i^4 \rangle - 2\langle n_i^3 \rangle + \langle n_i^2 \rangle) + \sum_i \sum_{j \neq i} N^{(4)} p_i^2 p_j^2 \quad (31)$$

Using the expression for the moments Eqs. 26-28, and noting that  $\sum_{j \neq i} p_j^2 = \sum_j p_j^2 - p_i^2 = p_C - p_i^2$ , we obtain

$$4N^{(3)} \sum_i p_i^3 + 2N^{(2)} p_C + N^{(4)} p_C^2. \quad (32)$$

Plugging this numerator into Eq. 29 we obtain after some algebra,

$$\text{Var}(\hat{p}_C) = \frac{4N^{(3)} \sum_i p_i^3 - 2N^{(2)}(2N-3)p_C^2 + 2N^{(2)}p_C}{(N(N-1))^2}, \quad (33)$$

the expression first published by Simpson [1].

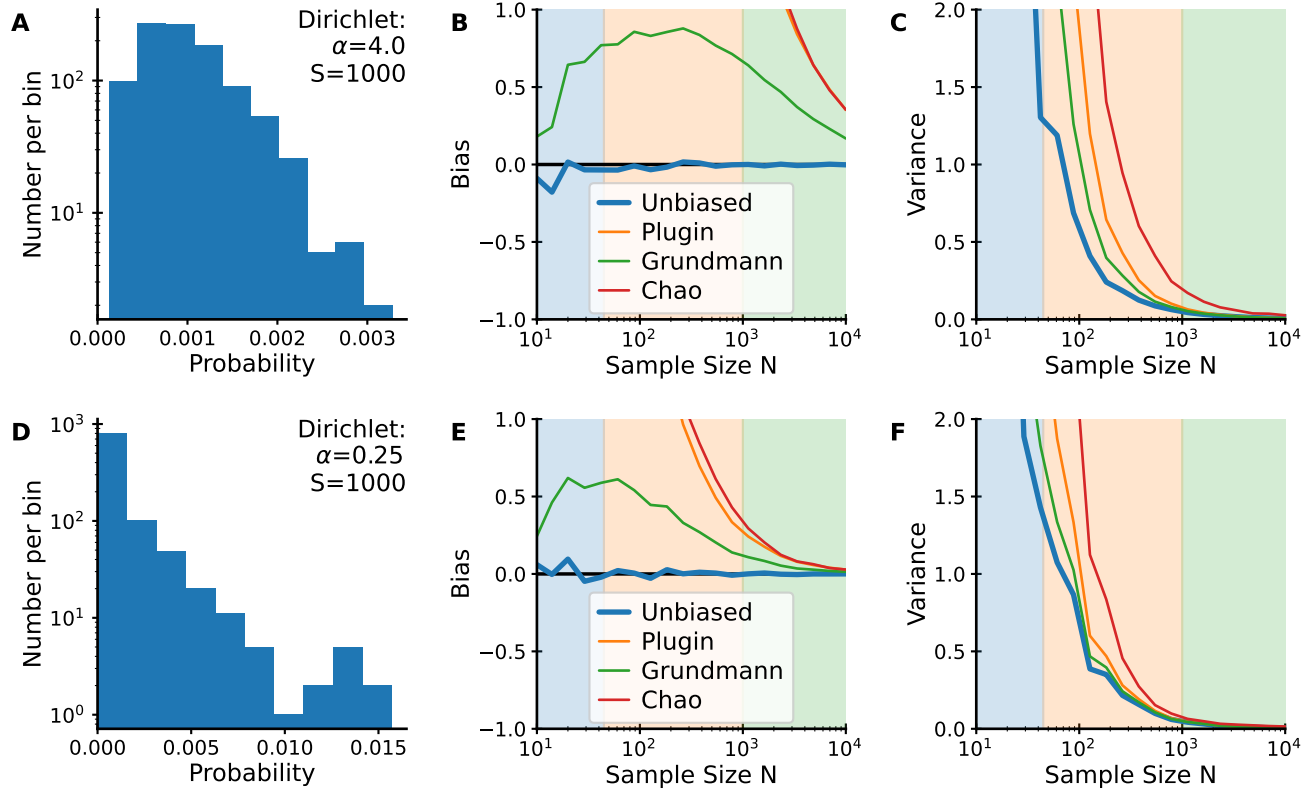


FIG. S1: **Supplement to Fig. 2.** Performance of variance estimators for species abundances drawn from a Dirichlet distribution with other choices of the parameter  $\alpha$ . Top:  $\alpha = 4.0$ . Bottom:  $\alpha = 0.25$ .

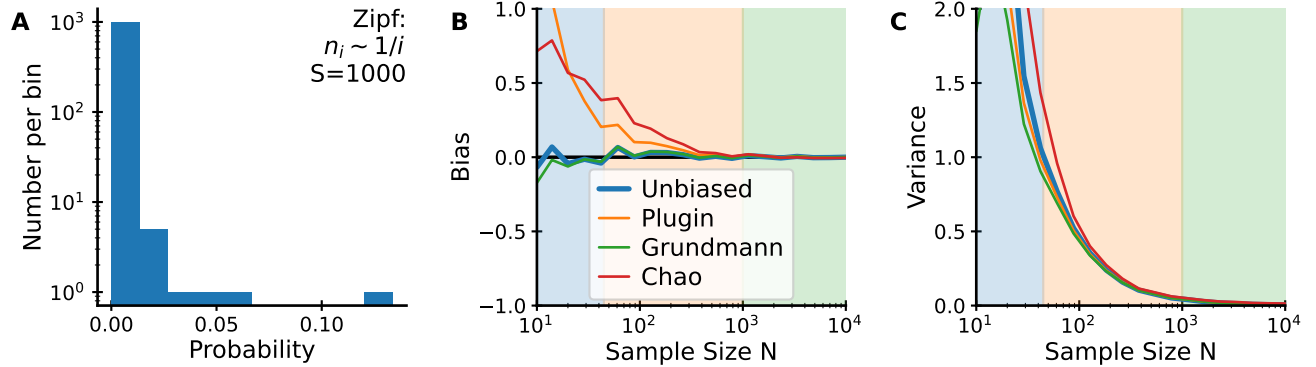


FIG. S2: **Supplement to Fig. 2.** Performance of variance estimators for a Zipf-distributed species abundances with  $p_i \sim 1/i$ .